Super-Resolution Target Localization by Fusing Signals from Multiple MIMO FMCW Automotive Radars

Zhang, Jiadi; Wang, Jianping; Yarovoy, Alexander

DOI
10.1049/icp.2024.1482

Publication date
2023

Document Version
Final published version

Published in
IET Conference Proceedings

Super-Resolution Target Localization by Fusing Signals from Multiple MIMO FMCW Automotive Radars

Jiadi Zhang, Jianping Wang, Alexander Yarovoy

Microwave Sensing, Signals and Systems (MS3)
Delft University of Technology (TU Delft), Delft, the Netherlands
jiadizhang0919@163.com, j.wang-4@tudelft.nl, a.yarovoy@tudelft.nl

Keyword: Super-resolution, Joint range-DOA estimation, FMCW, MIMO, Automotive radar

Abstract

Achieving high azimuth resolution is one of the main bottleneck for automotive radars, which generally demands a large aperture of antenna array. However, building an automotive radar system with a large antenna array is a very challenging task from the perspective of both technological readiness and cost. To circumvent this problem, we propose to fuse signals from multiple small automotive radars placed over the facade of a car as an alternative solution with low system complexity, where each radar with a small Multiple-Input Multiple-Output (MIMO) array operate independently without accurate synchronization. To (partially) coherently process the measurements from all the radars, a 2-D MUltiple Signal Classification (MUSIC) based algorithm is proposed for joint Direction-of-Arrival (DOA)-range estimation of targets in which spatial smoothing technique is exploited to tackle highly correlated signals. Taking advantage of the proposed estimation approach and multiple radars, it significantly improves the azimuth resolution of the system compared to that of a single MIMO radar. The performance of the proposed method is demonstrated through both numerical simulations and experimental results.

1 Introduction

Due to its advantages of day-and-night all-weather sensing capabilities, automotive radar plays an increasingly key role in Advanced Driver Assistance Systems(ADAS)/autonomous driving. To precisely detect and classify different targets in the environment, high spatial resolutions, including both down-range and (azimuth and elevation) angular resolutions, are of highly demand for automotive radars. To achieve high-range resolution, wideband (up-to 4 GHz bandwidth) signals can be used. Meanwhile, for high angular resolution, antenna arrays of large apertures are theoretically required; however, to build automotive radars with large antenna arrays is still a great challenge in terms of both technical feasibility and system cost. Although Multiple-Input-Multiple-Output (MIMO) array technique is used to reduce the complexity and cost of the radar system, the limited number of transmitting and receiving channels (i.e., 2×4 or 3×4) of the state-of-the-art automotive radar chips substantially constrains the achievable effective aperture of antenna arrays, leading to low angular resolution, i.e., $> 10^{\circ}$.

To overcome the technical bottleneck of angular resolutions of automotive radars, designing sophisticated MIMO arrays with increased number of transmitting and receiving channels combined with advanced super-resolution algorithms development for Direction-of-Arrival (DOA) estimation is the key solution. To increase the number of transmitting and receiving channels of the radar systems, one common idea in industry is to cascade multiple radar chips as a large system; thus, by fully exploiting the increased transmitting and receiving channels, MIMO arrays with a large effective aperture can be designed to achieve high-angular resolution. However, the chip cascading increases system complexity of the radar system and requires complicated calibration for coherent radar measurement, which proposes a great challenge to massive production. In addition, such radars do not fit easily in the modern autos' facade.

Accounting for the current angular-resolving challenge of automotive radars as well as the fact that multiple radars, at least two corner radars and one forward-looking radar, would be equipped along the facade of autonomous vehicles, we propose to fuse the signals from the multiple radars to enhance the angular resolution, especially, the azimuth resolution. To our best knowledge, the signal fusion of multiple MIMO radars for high-resolution DOA estimation has scarcely been reported in open literature. Hence, in this paper, the signal fusion of multiple automotive radars is studied.

Although some super-resolution approaches, such as MUltiple Signal Classification (MUSIC)-based approaches [1]–[3], Discrete-Fourier Transform (DFT)-MUSIC based methods [4], [5], Estimation of Signal Parameters via Rotational Invariance Technique (ESPRIT)-based method [6], [7], have been devel-

https://doi.org/10.1049/icp.2024.1482

oped for targets' DOA estimation/localization with MIMO-array based radars, they are mainly applicable to the radar systems with a single antenna array. For the radar systems consists of multiple MIMO antenna arrays, data association is required after targets' localization with respect to each individual array, which is generally not an easy task.

Meanwhile, for passive locally coherent arrays, Generalized MUSIC (GMUSIC) method proposed in [8] estimates source positions through synthesizing signal subspaces of all arrays in together. The number of targets is required as prior information. This method can resolve ambiguities in source localization compared with the decentralized MUSIC algorithm introduced in [9]. The direct position determination (DPD) method ([10], [11]) utilize observations from all arrays together, and the cost function only depends on source positions. Initially, [10] proposed the DPD algorithm based on maximum likelihood (ML), after that [11] combined DPD with MUSIC to save computational cost. However, this method is not suitable for chirp signals.

So, to fill the gap of signal fusion of multiple automotive radars, a novel super-resolution approach based on the MUSIC technique is developed to jointly estimate the DOAs and ranges of multiple targets. The proposed approach is generally applicable to fuse signals from multiple MIMO arrays arranged with a general topology.

The rest of the paper is organized as follows. In section 2, the FMCW radar system model is introduced, subsequently, signal model for monostatic configuration is analyzed. In section 3, the generalized 2D-MUSIC algorithm is developed. The performance of the proposed algorithm is analyzed via numerical simulations in section 4. Conclusions are drawn in section 5.

2 System Model

2.1 Geometrical Configuration

Without loss of generality, assume that there are $N_{\mathrm{r}} = 2M + 1$ identical FMCW MIMO radars in the system, where each radar has a MIMO array with N_{Tx} transmit and N_{Rx} receive antenna elements [12]. They are uniformly placed along the azimuth, as illustrated in Fig. 1. Within each small MIMO array, the inter-element spacing of receive antennas is $d_{\mathrm{Rx}} = \lambda/2$ (λ is the wavelength of the centre frequency) while the spacing between transmit antennas is $d_{\mathrm{Tx}} = N_{\mathrm{Rx}} d_{\mathrm{Rx}}$; thus the aperture size of the virtual array of a single MIMO array is $(N_{\mathrm{Tx}} N_{\mathrm{Rx}} - 1) d_{\mathrm{Rx}}$. Besides, the distance between two adjacent MIMO radars is $d_{\mathrm{s}} = \Delta \cdot d_{\mathrm{Rx}}$, where $d_{\mathrm{s}} \gg d_{\mathrm{Rx}}$. For the convenience of notation, we use the MIMO radar in the middle (indexed as the 0^{th} radar in Fig. 1) as a reference unit of the system. The small MIMO radar units in the system operate without synchronization.

For a typical automotive radar unit, the effective aperture size of the small MIMO array is just a few wavelength of the centre frequency (i.e., 77 GHz). Thus, the far-field assumption of the wave field radiation is generally used for

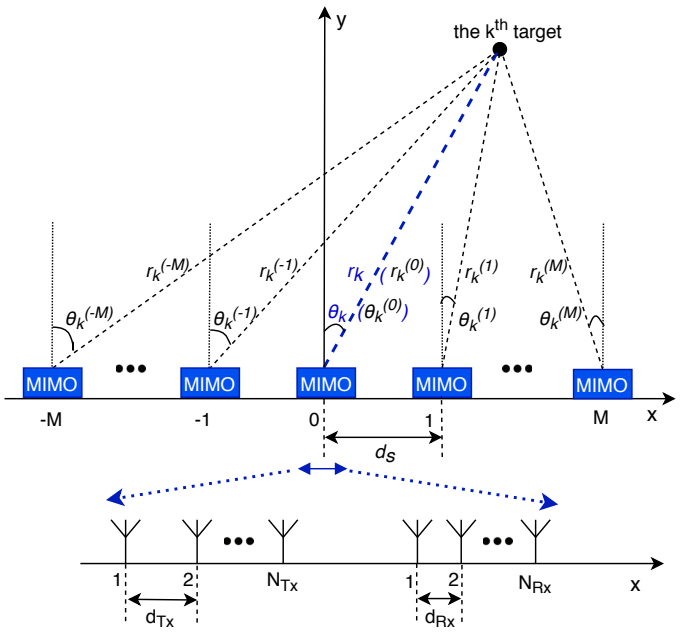

Fig. 1 Illustration of the geometrical model of the radar system

targets in a moderate distance, for instance, of dozens to hundreds of meters. However, when multiple MIMO radars are arranged as in Fig. 1, the aperture size formed by them significantly increases. Specifically, if the aperture size of one meter is formed for a radar system at 77 GHz, the far field approximation to the wavefront of the antenna array would be only valid beyond a distance of half a kilometer, which is much larger than the typical detection range of an automotive radar. So, for accurate estimation of targets' positions, we suggest using the near-field radiation model for the whole radar system while keep the far-field assumption for small MIMO arrays related to each radar unit. That is to say, the wavefronts of back-scattered signals are spherical from the system perspective, while they would be approximately treated as plane waves for each MIMO [13].

Assume that K stationary or slow moving point targets are located in the observation region and they can be observed by all radar units within the system. Targets' locations are parameterized with their ranges and DOAs relative to the reference radar unit as

$$\mathbf{r} = [r_1, r_2, \ldots, r_K] \tag{1}$$

$$\theta = [\theta_1, \theta_2, \ldots, \theta_K] \tag{2}$$

The ranges and DOAs of all targets relative to the m^{th} MIMO radar unit is denoted as

$$\mathbf{r}^{(m)} = \left[r_1^{(m)}, r_2^{(m)}, \ldots, r_K^{(m)}\right] \tag{3}$$

$$\theta^{(m)} = \left[\theta_1^{(m)}, \theta_2^{(m)}, \ldots, \theta_K^{(m)}\right] \tag{4}$$

where $m = -M, \ldots, M$ and $k = 1, \ldots, K$ denote the indices of the MIMOs and indices of the targets, respectively.

According to the geometry in Fig. 1, the distance $r_k^{(m)}$ between the k^{th} target and the m^{th} MIMO can be written as

$$r_k^{(m)} = \sqrt{r_k^2 + (md_{\text{s}})^2 - 2r_k md_{\text{s}} \sin(\theta_k)} \tag{5}$$

and the corresponding direction of departure (DOD) $\psi_k^{(m)}$ and DOA $\theta_k^{(m)}$ are

$$\psi_k^{(m)} = \theta_k^{(m)} = \arcsin\left(\frac{r_k \sin(\theta_k) - md_{\text{s}}}{r_k^{(m)}}\right) \tag{6}$$

where $\theta_k \in [-\pi/2, \pi/2]$.

2.2 Signal Model

For an FMCW radar with the deramping receiver, the acquired beat signal from the K stationary/slow-moving point targets in the illuminated scene can be expressed as:

$$x(t) = \sum_{k=1}^{K} \gamma_k \exp\left[j2\pi\left(\mu\tau_k t - f_0\tau_k - \frac{1}{2}\mu\tau_k^2\right)\right] + w(t) \tag{7}$$

where γ_k is the complex amplitude of the signal reflected by the k^{th} target. $\tau_k = 2r_k/c$ is the roundtrip time delay induced by the wave propagation between the k^{th} target and the antenna with a distance of r_k. f_0 is the initial frequency of the FMCW sweep and $\mu = B/T_s$ is the chirp rate of the FMCW sweep with the bandwidth B and the sweep duration T_s. $w(t) \sim \mathcal{CN}(0, \sigma^2)$ is the complex additive white Gaussian noise (AWGN) with the variance σ^2.

The beat signal in (7) is generally sampled by an Analogy to Digital Converter (ADC) at the sampling rate of f_s, and then the acquired discrete signal in a single sweep is given by

$$x[n] = \sum_{k=1}^{K} \gamma_k \exp\left[j2\pi\left(\mu\tau_k \frac{n}{f_s} - f_0\tau_k - \frac{1}{2}\mu\tau_k^2\right)\right] + w[n] \tag{8}$$

where $n = 0, \ldots, N-1$, and $N = \lfloor T_s \cdot f_s \rfloor$ is the number of samples in a sweep, where $\lfloor a \rfloor$ denotes the maximum integer that is not larger than a.

Considering the technological difficulty of phase synchronization among the multiple MIMO radar units, here we consider that each MIMO radar unit within the system operates separately in the monostatic configuration. Namely, each MIMO radar unit measures the scattered signals resulting from its own transmissions. The virtual antenna array of each MIMO radar unit is a uniform linear array (ULA) with $P = N_{\text{Tx}}N_{\text{Rx}}$ elements, and the spacing between two adjacent elements is $d = d_{\text{Rx}}$ [14]. Hence, the time delay varies linearly for consecutive elements in the virtual ULA. Since the MIMO radar unit used in the experiment has an even number of receiving antennas, we assume that $P = 2Q$, but the system model is also applicable if $P = 2Q + 1$. Fig. 2 shows the virtual ULA geometry of each MIMO, where the 0^{th} antenna is the reference antenna.

Taking advantage of the virtual array of each MIMO unit, the signals acquired by a small MIMO array is equivalent to that measured by the corresponding virtual ULA. So the

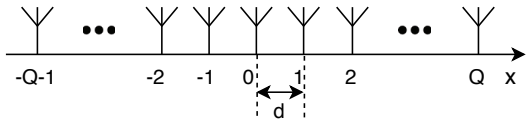

Fig. 2 Virtual ULA geometry of a MIMO

received signal by the q^{th} element of the virtual array of the m^{th} MIMO, in a single sweep duration, can be represented as

$$x_m[q,n] = \sum_{k=1}^{K} \gamma_k \exp\left[j2\pi\left(\mu\tau_k^{(m)}\frac{n}{f_s} - f_0\tau_k^{(m)} - \frac{1}{2}\mu\left(\tau_k^{(m)}\right)^2 + f_0\frac{qd\sin(\theta_k^{(m)})}{c}\right)\right] + w_m[q,n] \tag{9}$$

where $q = -Q-1, \ldots, 0, \ldots, Q$, and $\tau_k^{(m)} = 2r_k^{(m)}/c$ represents the roundtrip time delay caused by the distance $r_k^{(m)}$ between the m^{th} MIMO and the k^{th} target. Parameterizing the location of the k^{th} target with r_k and θ_k relative to the reference MIMO, then $r_k^{(m)}$ and $\theta_k^{(m)}$ can be obtained from r_k and θ_k through (5) and (6). Stacking all the measurements in (9), we get a data matrix $\mathbf{X}_m \in \mathbb{C}^{P\times N}$ that is given by

$$\mathbf{X}_m = [\mathbf{x}_m[-Q-1],\ \mathbf{x}_m[-Q],\ \cdots,\ \mathbf{x}_m[Q]]^T \tag{10}$$

where

$$\mathbf{x}_m[k] = [x_m[k,0],\ x_m[k,1],\ \cdots,\ x_m[k,N-1]]^T \in \mathbb{C}^N.$$

3 Generalized 2D-MUSIC Algorithm for Joint Range-DOA Estimation

3.1 Joint Range-DOA Estimation with Single MIMO Radar

For the m^{th} MIMO radar, its acquired signal can be stacked in a data matrix $\mathbf{X}_m \in \mathbb{C}^{P\times N}$ (as shown in Fig. 3), and then it is used as the input for range and angular estimation. However, when received signals are highly correlated or coherent, the rank of signal subspace would be deficient. To restore the rank of the signal covariance matrix, the forward-backward spatial smoothing (FBSS) technique [15] is generally employed. As the virtual array of each MIMO radar in the monostatic configuration is a ULA and the signal samples are sampled uniformly within each sweep (i.e., fast time), 2D-FBSS is applied along both spatial and time dimensions for each ULA. We define a window of dimensions $[l_1 \times l_2]$, where $K < l_1 < P$ and $K < l_2 < N$, and then scan the data matrix in all possible positions (see Fig. 3). Then, we have $p_1 = P - l_1 + 1$ sliding positions in the spatial dimension and $p_2 = N - l_2 + 1$ sliding positions in the time dimension.

For each sliding position $\tilde{\mathbf{p}} = (\tilde{p}_1, \tilde{p}_2)$, the sub-matrix $\mathbf{D}_m \in \mathbb{C}^{l_1\times l_2}$ is

$$\mathbf{D}_m(\tilde{\mathbf{p}}) = [\mathbf{x}_m(\tilde{p}_2), \mathbf{x}_m(\tilde{p}_2+1), \cdots, \mathbf{x}_m(\tilde{p}_2+l_2-1)] \tag{11}$$

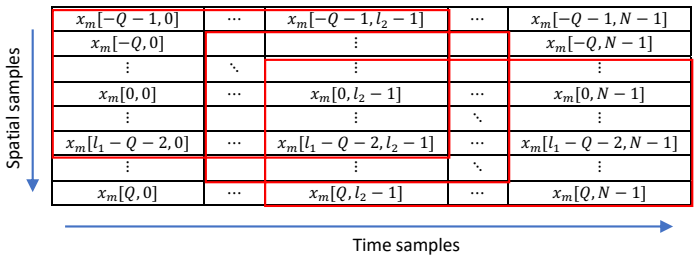

Fig. 3 Data matrix of the m^{th} MIMO with sliding window

where $\tilde{p}_1 = 0, 1, \cdots, P - l_1$, $\tilde{p}_2 = 0, 1, \ldots, N - l_2$ and

$$\mathbf{x}_m(\tilde{p}_2) = \begin{bmatrix} x_m(\tilde{p}_1 - Q - 1, \tilde{p}_2) \\ \vdots \\ x_m(\tilde{p}_1, \tilde{p}_2) \\ \vdots \\ x_m(\tilde{p}_1 + l_1 - Q - 2, \tilde{p}_2) \end{bmatrix} \in \mathbb{C}^{l_1 \times 1} \tag{12}$$

Each sub-matrix is reshaped into a vector of $l_1 l_2 \times 1$ by stacking its columns one by one, as

$$\begin{aligned} \mathbf{d}_m(\tilde{\mathbf{p}}) &= \text{vec}(\mathbf{D}_m(\tilde{\mathbf{p}})) \\ &= \left[\mathbf{x}_m(\tilde{p}_2)^{\text{T}}, \mathbf{x}_m(\tilde{p}_2 + 1)^{\text{T}}, \cdots, \mathbf{x}_m(\tilde{p}_2 + l_2 - 1)^{\text{T}}\right]^{\text{T}} \end{aligned} \tag{13}$$

and then collected into a new data matrix $\tilde{\mathbf{D}}_m \in \mathbb{C}^{l_1 l_2 \times p_1 p_2}$.

Then, the smoothed covariance matrix $\mathbf{R}_m \in \mathbb{C}^{l_1 l_2 \times l_1 l_2}$ can be obtained as [1]

$$\begin{aligned} \mathbf{R}_m &= \frac{1}{2p_1 p_2}\left[\tilde{\mathbf{D}}_m \tilde{\mathbf{D}}_m^{\text{H}} + \mathbf{J}(\tilde{\mathbf{D}}_m \tilde{\mathbf{D}}_m^{\text{H}})^* \mathbf{J}\right] \\ &= \mathbf{A}_{\text{s}}^{(m)} \mathbf{R}_{\text{s}}^{(m)} (\mathbf{A}_{\text{s}}^{(m)})^{\text{H}} + \sigma^2 \mathbf{I} \end{aligned} \tag{14}$$

where $\mathbf{J} \in \mathbb{C}^{l_1 l_2 \times l_1 l_2}$ is a reflection matrix

$$\mathbf{J} = \begin{bmatrix} 0 & 0 & \cdots & 1 \\ \vdots & 0 & 1 & 0 \\ 0 & \iddots & 0 & \vdots \\ 1 & 0 & \cdots & 0 \end{bmatrix}, \tag{15}$$

$\mathbf{R}_{\text{s}}^{(m)} \in \mathbb{C}^{K \times K}$ is the covariance matrix of received signals (excluding noise), and columns of $\mathbf{A}_{\text{s}}^{(m)} \in \mathbb{C}^{l_1 l_2 \times K}$ contain steering vectors of all targets

$$\mathbf{A}_{\text{s}}^{(m)} = [\mathbf{a}_m(r_1, \theta_1), \cdots, \mathbf{a}_m(r_K, \theta_K)] \tag{16}$$

The steering vector of the k^{th} target relative to the m^{th} MIMO can be expressed as

$$\mathbf{a}_m(r_k, \theta_k) = \mathbf{a}_m^{(r)}\left(r_k^{(m)}\right) \otimes \mathbf{a}_m^{(\theta)}\left(\theta_k^{(m)}\right) \tag{17}$$

where r_k and θ_k describes the location of the k^{th} target relative to the reference MIMO. $\mathbf{a}_m^{(r)} \in \mathbb{C}^{l_2 \times 1}$ and $\mathbf{a}_m^{(\theta)} \in \mathbb{C}^{l_1 \times 1}$ are steering vectors of the range $r_k^{(m)}$ and DOA $\theta_k^{(m)}$ for the k^{th} target relative to the m^{th} MIMO radar, respectively. The relations between $r_k^{(m)}, \theta_k^{(m)}$ and r_k, θ_k are given by (5) and (6).

From the signal model in (9), we can write the range and DOA steering vectors $\mathbf{a}_m^{(r)}$ and $\mathbf{a}_m^{(\theta)}$ in (17) as

$$\mathbf{a}_m^{(r)}\left(r_k^{(m)}\right) = \left[1, \cdots, \exp\left(j2\pi\mu \frac{2r_k^{(m)}}{c}\frac{l_2 - 1}{f_s}\right)\right]^{\text{T}} \tag{18}$$

$$\begin{aligned} \mathbf{a}_m^{(\theta)}\left(\theta_k^{(m)}\right) = \Bigg[&\exp\left(j2\pi f_0 \frac{(-Q-1)d\sin(\theta_k^{(m)})}{c}\right), \\ &\cdots, \exp\left(j2\pi f_0 \frac{(l_1 - Q - 2)d\sin(\theta_k^{(m)})}{c}\right)\Bigg]^{\text{T}} \end{aligned} \tag{19}$$

Applying eigenvalue decomposition (EVD) or singular value decomposition (SVD) to the smoothed covariance matrix $\mathbf{R}_m$, one can get

$$\mathbf{R}_m = \mathbf{U}_{\text{s}}^{(m)} \mathbf{\Sigma}_{\text{s}}^{(m)} \left(\mathbf{U}_{\text{s}}^{(m)}\right)^{\text{H}} + \mathbf{U}_{\text{n}}^{(m)} \mathbf{\Sigma}_{\text{n}}^{(m)} \left(\mathbf{U}_{\text{n}}^{(m)}\right)^{\text{H}} \tag{20}$$

where $\mathbf{U}_{\text{s}}^{(m)} \in \mathbb{C}^{l_1 l_2 \times K}$ is the signal subspace that contains eigenvectors of the K largest eigenvalues $\mathbf{\Sigma}_{\text{s}}^{(m)} \in \mathbb{C}^{K \times K}$, and $\mathbf{U}_{\text{n}}^{(m)} \in \mathbb{C}^{l_1 l_2 \times (l_1 l_2 - K)}$ is the noise subspace which includes eigenvectors of the $(l_1 l_2 - K)$ smallest eigenvalues $\mathbf{\Sigma}_{\text{n}}^{(m)} \in \mathbb{C}^{(l_1 l_2 - K) \times (l_1 l_2 - K)}$.

The columns of $\mathbf{A}_{\text{s}}^{(m)}$ in (14) span the same space as the columns of signal subspace $\mathbf{U}_{\text{s}}^{(m)}$ in (20). However, $\mathbf{A}_{\text{s}}^{(m)}$ and $\mathbf{U}_{\text{n}}^{(m)}$ are not perfectly orthogonal to each other due to the influence of noise. Thus, targets' positions are generally estimated by minimizing the following objective function,

$$\arg\min_{r,\theta} \quad \mathbf{a}_m^{\text{H}}(r, \theta) \mathbf{U}_{\text{n}}^{(m)} \left(\mathbf{U}_{\text{n}}^{(m)}\right)^{\text{H}} \mathbf{a}_m(r, \theta) \tag{21}$$

To address the minimization problem in (21), grid search can be used. A search grid can be defined over the domain of possible targets' locations (i.e., range-angular domain) with respect to the reference MIMO radar. Then, the search grid for each MIMO radar can be obtained through (5) and (6). After that, using the principle of MUSIC approach, the minimization problem in (21) for joint range-DOA estimation can be converted to evaluate the following 2D pseudo-spectrum $f_m(r, \theta)$ for the m^{th} MIMO radar

$$f_m(r, \theta) = \frac{1}{\mathbf{a}_m^{\text{H}}(r, \theta) \mathbf{U}_{\text{n}}^{(m)} \left(\mathbf{U}_{\text{n}}^{(m)}\right)^{\text{H}} \mathbf{a}_m(r, \theta)} \tag{22}$$

where $\mathbf{a}_m(r, \theta)$ is the steering vector for a possible target's position to the m^{th} MIMO, which is defined in (17). Through the grid search, the associated parameters of the spikes of $f_m(r, \theta)$ indicates the estimated positions of targets.

3.2 Signal Fusion of Multiple MIMO Radars for Super-resolution Range-DOA Estimation

In this subsection, signal fusion of multiple MIMO radars is discussed to improve the (azimuth) angular resolution of targets' position estimation. For a radar system consisting of N_{r} identical small MIMO arrays (as shown in Fig. 1), the phase histories of scattered signals acquired by each MIMO arrays are connected via their geometrical relations;

thus, one can take advantage of the relations among scattered signals acquired by each MIMO radar and jointly construct the noise subspace and steering vectors for high-resolution DOA estimation [8].

Since the system contains N_r identical MIMOs, we have to integrate estimation results of all virtual arrays to obtain the final result. The same search grid is applied to all virtual arrays to maintain geometrical constraints, which includes all potential targets' positions parameterized with the range r and DOA θ relative to the reference MIMO. Then the search grid can be transferred for each MIMO via (5) and (6).

Virtual arrays in the system do not share measured data samples with one another, which means every virtual array can do estimation individually. Nevertheless, our main objectives are to improve azimuth resolution and get robust estimation result by jointly using multiple MIMOs. We prefer to coherently integrate all virtual arrays during the search stage instead of fusing individual estimation results. Therefore, we jointly constructs the noise subspace and steering vectors based on the geometrical relations among different MIMOs [8].

The generalized 2D-MUSIC spatial spectrum function for integrating all virtual arrays in monostatic configuration can be written as

$$f(r,\theta) = \frac{1}{\mathbf{a}^{\mathrm{H}}(r,\theta)\mathbf{U}_n\mathbf{U}_n^{\mathrm{H}}\mathbf{a}(r,\theta)} \tag{23}$$

where $\mathbf{a}(r,\theta) \in \mathbb{C}^{N_\mathrm{r} l_1 l_2 \times 1}$ and $\mathbf{U}_n \in \mathbb{C}^{N_\mathrm{r} l_1 l_2 \times N_\mathrm{r}(l_1 l_2 - K)}$ are joint steering vector and noise subspace of the system, respectively.

The joint steering vector $\mathbf{a}(r,\theta)$ can be expressed as:

$$\mathbf{a}(r,\theta) = [\mathbf{a}_{-M}(r,\theta);\ldots;\mathbf{a}_m(r,\theta);\ldots;\mathbf{a}_M(r,\theta)] \tag{24}$$

The joint noise subspace $\mathbf{U}_n$ is constructed as:

$$\mathbf{U}_n = \begin{bmatrix} \mathbf{U}_n^{(-M)} & \mathbf{0} & \cdots & \cdots & \mathbf{0} \\ \mathbf{0} & \ddots & \ddots & & \vdots \\ \vdots & \mathbf{0} & \mathbf{U}_n^{(m)} & \mathbf{0} & \vdots \\ \vdots & & \ddots & \ddots & \mathbf{0} \\ \mathbf{0} & \cdots & \cdots & \mathbf{0} & \mathbf{U}_n^{(M)} \end{bmatrix} \tag{25}$$

where $m = -M,\ldots,M$.

Simplifying (23), one can get

$$\begin{aligned} f(r,\theta) &= \left(\sum_{m=-M}^{M} \mathbf{a}_m(r,\theta)^{\mathrm{H}} \mathbf{U}_n^{(m)} (\mathbf{U}_n^{(m)})^{\mathrm{H}} \mathbf{a}_m(r,\theta) \right)^{-1} \\ &= \left(\sum_{m=-M}^{M} f_m^{-1}(r,\theta) \right)^{-1} \end{aligned} \tag{26}$$

where $f_m(r,\theta)$ is defined in (22).

Note that when there is only a single MIMO, (26) is simplified to the traditional 2D-MUSIC algorithm.

4 Numerical Simulations

To emulate the forward-looking radar and two corner radars in the facade of an autonomous vehicle, an automotive radar system consisting of three small identical coherent FMCW MIMO radar is considered. The three MIMO radars are placed along a line with inter-spacings of $d_\mathrm{s} = 0.5\,\mathrm{m}$ and operate in the monostatic configuration. Each small MIMO radar operates at the centre frequency of $f_c = 76.5\,\mathrm{GHz}$ and has two transmitters and four receivers, which results in a virtual ULA with the inter-element spacings of $d = \lambda/2$. Without explicit declariation, the configurations of radar system above are used for both point and extended target simulations below.

4.1 Point Targets Simulations

Point targets simulation is presented in this section. The signal bandwidth of the FMCW radars is $B = 600\,\mathrm{MHz}$ and the sweep duration is $T = 60\,\mu\mathrm{s}$. In each sweep, $N = 372$ time samples are acquired with sampling frequency $f_s = 6.2\,\mathrm{MHz}$. Three point targets are set in the observation scene, where two of them are placed in the same range while two of them locates in the same bearing direction relative to the composed radar system. Targets' ranges and azimuth angles are $(19.95\,\mathrm{m}, -2.4^\circ)$, $(19.95\,\mathrm{m}, 3^\circ)$ and $(20.2\,\mathrm{m}, 3^\circ)$. The synthetic radar data is generated with the signal to noise rate (SNR) of $15\,\mathrm{dB}$ in all simulations.

By taking advantage of the generalized 2-D MUSIC algorithm with the search grid of $\Delta R = 0.02\,\mathrm{m}$ and $\Delta\theta = 0.02^\circ$, respectively, in range and azimuth dimensions, the joint estimations of range and DOA of targets are obtained. Fig. 4 displays the pseudo spectra obtained with both a single MIMO and the composed system with three MIMO radars in the monostatic configuration. In both case, 2D-FBSS with sliding window size of $[5 \times 100]$ is employed along both spatial and time dimensions. Comparing Fig. 4 (a) with (b), one can see that azimuth resolution clearly improves with the composed system of three MIMO radars in the monostatic configuration (i.e., by fusing the signals from three MIMO radars). For better illustration, the angular slice of the pseudo-spectrum of the two point targets in the same range bin is shown in Fig. 5.

Meanwhile, Fig. 6 shows the range slice of the pseudo-spectrum of the two targets in the range bearing direction relative to the radar system. It is clear that both the single MIMO radar and the composed radar system achieve better down-range resolution compared with the Rayleigh range resolution $(\delta R = 0.25\,\mathrm{m})$.

4.2 Electromagnetic Simulation of Extended Target

A numerical experiment for an extended target is demonstrated in this section. The FMCW MIMO radar signal is generated in the frequency domain with the electromagnetic simulation software HFSS SBR+ with a full-scale car CAD model as an object. The radar signal bandwidth is set to be $B = 1\,\mathrm{GHz}$, the frequency step is $\Delta f = 2\,\mathrm{MHz}$ and the sweep duration is $T = 0.5\,\mu\mathrm{s}$. After modulating the generated data with proper

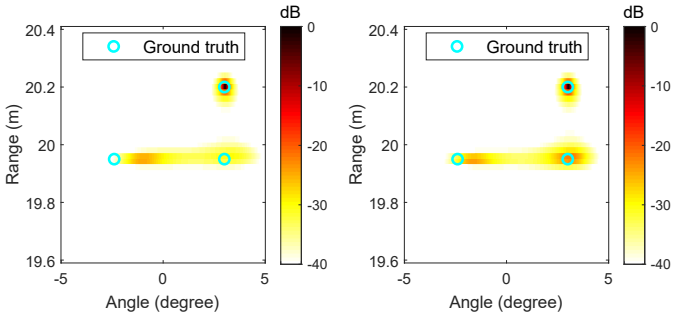

Fig. 4 Pseudo spectrum of three point targets when SNR is 15dB. (a) a single MIMO, (b) the composed radar system.

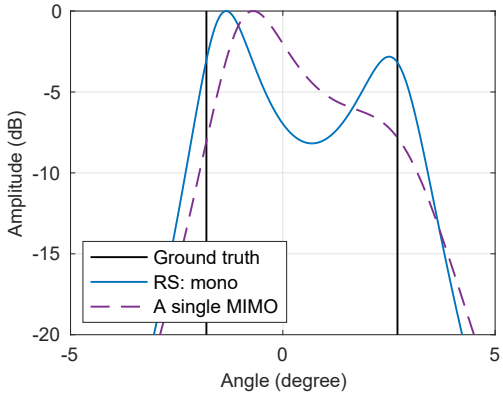

Fig. 5 Slices of pseudo spectra of a single MIMO and the composed radar system. Black line represents ground truth of targets' locations. The blue line represents slice of pseudo spectrum of the composed radar system. The purple dashed line represents slice of pseudo spectrum of a single MIMO.

group-time delays, the synthetic data is converted into the time domain to get targets' echo of FMCW radar. The equivalent sampling rate is $f_s = 154\,\mathrm{GHz}$ and then the downsampling factor is set to 100. Then the number of samples per chirp after downsampling is $N = 770$.

Fig. 7 illustrates the simulation setup of the extended target together with the radar system. The simulation scenario consists of a full-scale car CAD model and the ground. The relative down-range distance between the car and radar system is $20\,\mathrm{m}$. The inter-MIMO spacing is $0.5\,\mathrm{m}$. Elevation and azimuth beamwidths of each antenna are $20°$ and $120°$, respectively.

Fig. 8 displays the pseudo spectrum of the generalized 2D-MUSIC algorithm with a single MIMO and the monostatic configuration of the radar system. Although the 3D extended target is considered, the estimation results are, for convenience, displayed in a 2D coordinate. As the target is far away from the radar system, top view of the extended target can approximately describe the size of target indicated by the blue box in each plot. In addition, we set $-25\,\mathrm{dB}$ as the threshold

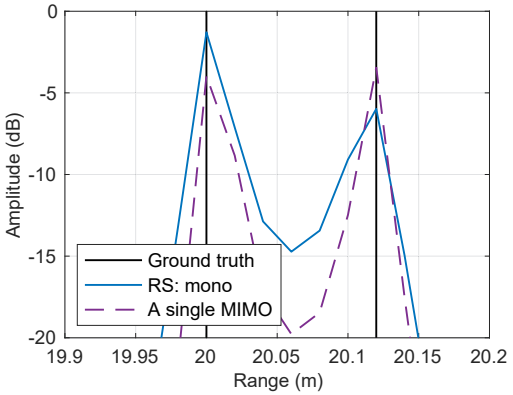

Fig. 6 Slices of pseudo spectra of a single MIMO and the composed radar system. Black line represents ground truth of targets' locations. The blue line represents slice of pseudo spectrum of the composed radar system. The purple dashed line represents slice of pseudo spectrum of a single MIMO.

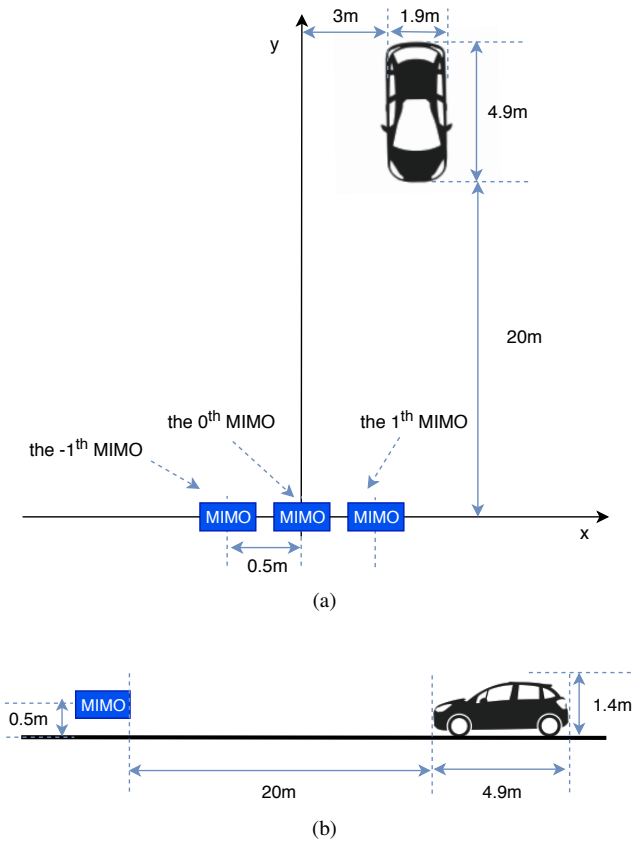

Fig. 7 Ground truth of an extended target with the radar system: (a) top view, (b) right view.

for the normalized singular values to estimate the number of targets for each virtual ULA. Then the maximum value is selected as the estimated number of targets. Strong reflection points are corresponding to the front side and wheels of the car. Fig. 8 indicates that the composed radar system with

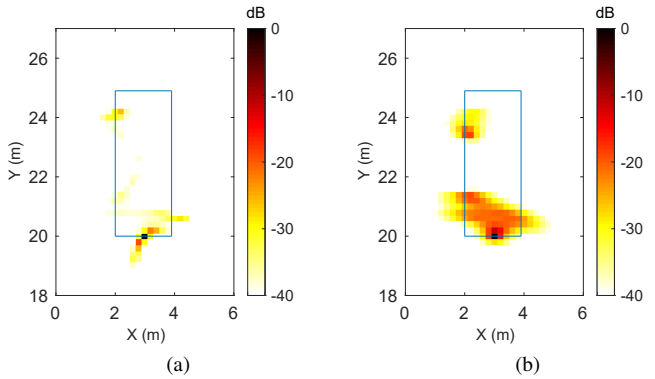

Fig. 8 Estimation results of an extended target with ground: (a) a single MIMO, (b) the composed radar system.

three MIMO arrays is helpful to extract more strong reflection points, and then the estimation obtains a better profile of the target.

5 Conclusions

In this paper, a novel methodology to improve the azimuth angular resolution of automotive radar is proposed by fusing the signals from multiple small MIMO radar systems placed along the facade of a vehicle. A generalized 2D-MUSIC algorithm is developed to fuse signals for super-resolution estimation of targets' DOAs. This proposed approach is also applicable for multistatic configuration of the radar system. Although the estimation accuracy of the proposed generalized 2-D MUSIC, similar to MUSIC, depends on the search grid, it can be improved by applying an iterative grid refinement method. In the implementation, the computational speed of the proposed approach can be significantly accelerated via proper parallel computing of the pseudo-spectrum related to each steering vector, which is attractive for practical usage of automotive radars.

References

[1] F. Belfiori, W. v. Rossum, and P. Hoogeboom, "Coherent music technique for range/angle information retrieval: application to a frequency-modulated continuous wave mimo radar," *IET Radar, Sonar Navigation*, vol. 8, no. 2, pp. 75–83, February 2014.

[2] F. Belfiori, W. van Rossum, and P. Hoogeboom, "Application of 2d music algorithm to range-azimuth fmcw radar data," in *2012 9th European Radar Conference*, Oct 2012, pp. 242–245.

[3] ——, "2d-music technique applied to a coherent fmcw mimo radar," in *IET International Conference on Radar Systems (Radar 2012)*, Oct 2012, pp. 1–6.

[4] S. Xu, J. Wang, and A. Yarovoy, "Super resolution doa for fmcw automotive radar imaging," in *2018 IEEE Conference on Antenna Measurements Applications (CAMA)*, Sep. 2018, pp. 1–4.

[5] S. Kim, Y. Ju, and J. Lee, "A low-complexity joint toas and aoas parameter estimator using dimension reduction for fmcw radar systems," *Elektronika ir Elektrotechnika*, vol. 24, 08 2018.

[6] D. G. Oh, Y. H. Ju, and J. H. Lee, "Subspace-based auto-paired range and doa estimation of dual-channel fmcw radar without joint diagonalisation," *Electronics Letters*, vol. 50, no. 18, pp. 1320–1322, August 2014.

[7] S. Kim, D. Oh, and J. Lee, "Joint dft-esprit estimation for toa and doa in vehicle fmcw radars," *IEEE Antennas and Wireless Propagation Letters*, vol. 14, pp. 1710–1713, 2015.

[8] D. W. Rieken and D. R. Fuhrmann, "Generalizing music and mvdr for multiple noncoherent arrays," *IEEE Transactions on Signal Processing*, vol. 52, no. 9, pp. 2396–2406, Sep. 2004.

[9] M. Wax and T. Kailath, "Decentralized processing in sensor arrays," *IEEE Transactions on Acoustics, Speech, and Signal Processing*, vol. 33, no. 5, pp. 1123–1129, October 1985.

[10] A. J. Weiss, "Direct position determination of narrowband radio frequency transmitters," *IEEE Signal Processing Letters*, vol. 11, no. 5, pp. 513–516, May 2004.

[11] A. Amar and A. J. Weiss, "Direct position determination of multiple radio signals," in *2004 IEEE International Conference on Acoustics, Speech, and Signal Processing*, vol. 2, May 2004, pp. ii–81.

[12] J. Zhang, "Super-resolution algorithms for target localization using multiple FMCW MIMOs," Master's thesis, Delft University of Technology, Delft, the Netherlands, Aug. 2019, available at http://resolver.tudelft.nl/uuid:6b671bde-80ca-4852-b626-dc290f0ab652.

[13] W. Zhi and M. Y. Chia, "Near-field source localization via symmetric subarrays," *IEEE Signal Processing Letters*, vol. 14, no. 6, pp. 409–412, June 2007.

[14] J. Li and P. Stoica, *MIMO Radar Signal Processing*, ser. Wiley - IEEE. Wiley, 2008.

[15] S. U. Pillai and B. H. Kwon, "Forward/backward spatial smoothing techniques for coherent signal identification," *IEEE Transactions on Acoustics, Speech, and Signal Processing*, vol. 37, no. 1, pp. 8–15, Jan 1989.